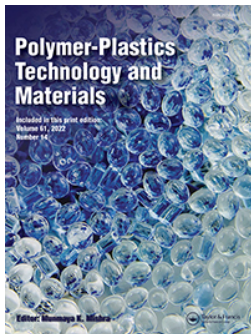


Polymer-Plastics Technology and Materials

Included in this print edition:
Volume 51, 2022
Number 10






Sulfonated polyaniline synthesis *via* moistureproof sulfonation of emeraldine salt polyaniline for graphite-based composite counter electrode in dye-sensitized solar cells

Muhammad Reza, Fauziah Nurfalah, Triannisa Rahmawati, Phutri Milana, Auliya Nur Amalina, Risa Rahmawati Sunarya, Fry Voni Steky & Veinardi Suendo

To cite this article: Muhammad Reza, Fauziah Nurfalah, Triannisa Rahmawati, Phutri Milana, Auliya Nur Amalina, Risa Rahmawati Sunarya, Fry Voni Steky & Veinardi Suendo (2022) Sulfonated polyaniline synthesis *via* moistureproof sulfonation of emeraldine salt polyaniline for graphite-based composite counter electrode in dye-sensitized solar cells, Polymer-Plastics Technology and Materials, 61:14, 1564-1577, DOI: [10.1080/25740881.2022.2071161](https://doi.org/10.1080/25740881.2022.2071161)



To link to this article: <https://doi.org/10.1080/25740881.2022.2071161>

 View supplementary material 

 Published online: 03 May 2022.

 Submit your article to this journal 

 Article views: 133

 View related articles 

 View Crossmark data 



Sulfonated polyaniline synthesis *via* moistureproof sulfonation of emeraldine salt polyaniline for graphite-based composite counter electrode in dye-sensitized solar cells

Muhammad Reza ^{a,b}, Fauziah Nurfalah^a, Triannisa Rahmawati^{a,c}, Phutri Milana ^a, Auliya Nur Amalina ^a, Risa Rahmawati Sunarya ^{a,d}, Fry Voni Steky ^a, and Veinardi Suendo ^{a,e}

^aDivision of Inorganic and Physical Chemistry, Faculty of Mathematics and Natural Sciences, Institut Teknologi Bandung, Bandung, Indonesia; ^bDepartment of Chemistry, Faculty of Mathematics and Natural Sciences, Universitas Jember, Jember, Indonesia; ^cChemistry Education Study Program Department of Chemistry Education, Faculty of Mathematics and Science Education, Indonesia University of Education, Bandung, Indonesia; ^dDepartment of Chemistry Education, Faculty of Tarbiyah and Teacher Training, UIN Sunan Gunung Djati Bandung, Bandung, Indonesia; ^eResearch Center for Nanoscience and Nanotechnology, Institut Teknologi Bandung, Bandung, Indonesia

ABSTRACT

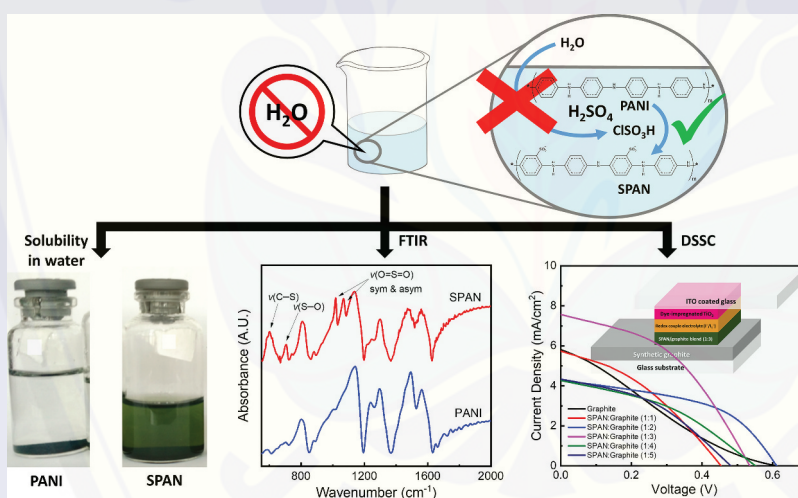
We demonstrated a room-temperature synthesis of nontoxic polar-solvent-soluble sulfonated polyaniline (SPAN). Polyaniline emeraldine salt (PANI ES) was used as starting material for a simple moistureproof sulfonation in producing SPAN. The optimum condition was obtained at a ClSO_3H concentration of 30% in sulfuric acid for 72 h of sulfonation. FTIR and Raman spectra revealed that the sulfonic group ($-\text{SO}_3\text{H}$) is covalently bonded to the PANI ES chain. Electrical conductivity measurement of SPAN provides the conductivity value within the semiconductor range. The obtained power conversion efficiency is twice higher than a graphite-based counter electrode due to the good electrocatalytic activity of SPAN.

ARTICLE HISTORY

Received 13 January 2022
Revised 18 April 2022
Accepted 21 April 2022

KEYWORDS

Sulfonated polyaniline; sulfonic group; electrical conductivity; counter electrode; dye-sensitized solar cell



1. Introduction

Dye-sensitized solar cells (DSSC) have been widely investigated as the next-generation solar cell due to their moderate efficiency of light-to-electricity conversion, simple device fabrication process, and low fabrication cost.^[1,2] Generally, there are three main components of DSSC: a dye-sensitized nanomaterial film electrode, a redox electrolyte, and a counter electrode.^[3,4] Titanium dioxide

(TiO_2) became the most commonly preferred semiconductor for photoanodes. It provides numerous advantages in sensitized photochemistry and photo-electrochemistry: it has a low-cost, widely available, withstand to acidic condition, nontoxic, and excellent biocompatibility as materials that can be employed in both health care and home applications. The conventional “state-of-the-art” dye is the ruthenium complex based dye, tris

CONTACT Veinardi Suendo vsuendo@chem.itb.ac.id Division of Inorganic and Physical Chemistry, Faculty of Mathematics and Natural Sciences, Institut Teknologi Bandung, Bandung, Indonesia

Supplemental data for this article can be accessed online at <https://doi.org/10.1080/25740881.2022.2071161>

© 2022 Taylor & Francis

(2,2'-bipyridyl-4,4-carboxylate) ruthenium(II), also known as N719, with the carboxylate as the chromophore's anchoring group to facilitate chemisorption to the oxide substrate.^[5] The iodide/triiodide couple has a good redox potential and provides rapid dye regeneration and slow electron recombination; at the same time, the couple has good solubility, high conductivity, and low light absorption, as well as favorable penetration ability into the mesoporous semiconductor film and long-term stability. The iodide/triiodide pair has been the favored redox couple since the beginning of DSSC development because of their unique characteristics.^[6] Because of its low viscosity, excellent solubility, and chemical durability (electrochemical window > 4 V), acetonitrile is regarded the most suitable electrolyte for fundamental studies of DSSC.^[7]

The counter electrode plays a vital role in collecting electrons and catalyzing the redox couple species' reduction in electrolytes.^[5, 8–10] In addition, it serves to transfer electrons from the external circuit to regenerate the redox couple in DSSC. Therefore, a high-performance DSSC requires a highly catalytic and conductive counter electrode. Currently, a transparent conducting oxide substrate coated by a layer of platinum (Pt) is usually used as a counter electrode of the DSSC to catalyze the I_3^- reduction to I^- in the I^-/I_3^- redox couple electrolyte.^[11,12] However, Pt is one of the rare noble metals, which remarkably increases the fabrication cost of DSSC. Therefore, many lower-cost alternative materials have been investigated as the counter electrode in DSSC to replace Pt.^[13] Several attempts on various carbon materials, like graphite, have been carried out to reduce the production cost of DSSC.^[14–16] Graphite is a potential electrode material due to its high conductivity and corrosion resistance toward couple-redox electrolytes. However, the conversion efficiency of the DSSC based on the graphite electrode is relatively low due to the insufficient catalytic activity for I_3^- reduction.^[17,18] Graphite is usually blended with another material with different functional groups to facilitate the redox reaction between the counter electrode and I^-/I_3^- redox couple electrolyte. Therefore, the combination of graphite and the conductive polymer is expected to improve the counter electrode performances. Conducting polymers are promising candidates as an additive for graphite-based counter electrode materials in DSSC due to their unique properties such as good stability and catalytic activity for I_3^- reduction.^[19,20]

During the last decades, polyaniline (PANI) has been one of the most intensively studied conducting polymers. PANI provides numerous synthesis methods, wide-range conductivity, good environmental stability, and interesting redox properties.^[21–23] The characteristics of PANI are suitable for photovoltaic

applications.^[24,25] Several works have shown PANI applications in DSSC to improve the carbon-based counter electrode's electrocatalytic activity.^[26–28] However, PANI is not readily soluble in common non-toxic polar solvents (i.e., water, alcohol, and ketone), leading to further processing difficulties. Sulfonated polyaniline (SPAN) is a self-doped water-soluble conductive polyaniline derivative.^[15, 29–35] SPAN is a primary model for the dopant and secondary dopant-induced processability in PANI, in addition to its self-doping nature.^[36] SPAN is a fascinating PANI derivative due to its extraordinary electroactive properties, improved processability, and numerous potential industrial applications.^[34,35,37] Therefore, the unique chemical reactivity, electroactivity, and excellent conductivity lead to the broad application potentials, i.e., CO_2 sensors,^[38] Schottky diodes,^[33] electron beam resists,^[32] anti-corrosion coatings,^[39] and Brønsted acid catalyst.^[40] However, there is no completed report of SPAN usage as a counter electrode in DSSC. Direct sulfonation in SPAN synthesis is challenging due to its rapid reaction, highly exothermic, and high sensitivity to humidity. Therefore, most controllable SPAN synthesis follows polymerization of metanilic acid or aniline/metanilic acid mixture.^[32,40] Commonly used sulfonating agents in direct sulfonation of polyaniline, i.e., emeraldine base, is fuming sulfuric acid.^[15,34,35,37]

This work reports the detailed synthesis of SPAN using a moistureproof sulfonation method. PANI's conductive form, the PANI emeraldine salt (PANI ES), was used as the starting material. Chlorosulfuric acid ($ClSO_3H$) in concentrated sulfuric acid (H_2SO_4) was used as the sulfonating agent. The concentration of $ClSO_3H$ in the sulfonating agent and sulfonation duration were also varied. The synthesized SPAN was then blended with graphite to produce the counter electrode materials for DSSC. We expect the photovoltaic performances of fabricated DSSC could be improved using an optimized SPAN:graphite blend counter electrode. SPAN is expected to enhance the electrocatalytic activity of graphite-based counter electrode.

2. Experimental

2.1. Materials

Aniline, acetone, hydrochloric acid (HCl), graphite, and sulfuric acid (H_2SO_4) were purchased from Sigma-Aldrich. Chlorosulfuric acid ($ClSO_3H$) and ammonium persulfate (APS) were obtained from Merck. All reagents with analytical grade were directly used without further purification except for aniline. Aniline was distilled to remove oligoaniline impurities prior to the polymerization processes.

The ruthenium complex dye, N719, was the commercially available product obtained from Solaronix. The ITO electrical conducting glasses ($R_s < 11 \Omega \text{ square}^{-1}$) were obtained from Kaivo Optoelectronic Technology, China.

2.2. Synthesis of PANI emeraldine salt (PANI ES)

PANI ES was synthesized by the method that has been reported before.^[41] First, we dissolved 1.82 mL of aniline in 50 mL of HCl 1 M as a first solution. Next, we dissolved 5.71 g of APS in 50 mL demineralized water as a second solution and put it in an ethylene glycol bath with a temperature of 0°C for 1 h. After that, the first solution was added to the second solution at the same temperature under vigorous stirring for 24 h. Finally, the reaction mixture was filtered, washed using acetone and HCl, and then dried under a dynamic vacuum for 24 h.

2.3. Synthesis of sulfonated polyaniline (SPAN)

10 mL of ClSO_3H and concentrated H_2SO_4 mixture was added to 0.2 g of PANI powder until it dissolved, and the color changed to dark red. The amount of ClSO_3H in concentrated H_2SO_4 was varied from 5 to 40% (v/v). The duration of sulfonation was also varied for 24, 48, and 72 h at room temperature under constant stirring (Table 1). The green paste separated on the bottom of the flask was precipitated by the addition of plenty of cold water. The precipitate was collected on a Buchner funnel, washed by cold water and acetone, respectively, and dried under a dynamic vacuum for 24 h.^[35]

2.4. Preparation of counter electrode and DSSC fabrication

SPAN:graphite paste was made by mixing SPAN and graphite with various compositions in a methylcellulose/glacial acetic acid mixture. SPAN's mass ratios to graphite used in this work are 1:1, 1:2, 1:3, 1:4, and 1:5, respectively. Each SPAN:graphite paste was deposited on a synthetic graphite-coated glass substrate using a common screen-print method as reported

elsewhere.^[42] The detailed schematic of the screen-print method performed in this study is depicted in Figure S1. The fabricated counter electrode was then heated at 120 °C for 15 min. With an active area of 0.81 cm², the photoanode was prepared by screen printing TiO_2 paste on the ITO glass substrate, followed by sintering at 500 °C for 1 h. The thickness of the active layer of both the fabricated counter electrode and photoanode was around 20 μm obtained by Mitutoyo SurfTest SJ-210 Profilometer.^[26] Next, the obtained TiO_2 photoanode was immersed into a 5×10^{-4} M Ruthenium complex dye (N719) solution for 20 h. The electrolyte used in this study was the I^-/I_3^- redox couple solution in acetonitrile. All components were assembled like a sandwich and held using two binder clips.

2.5. Characterizations

FTIR spectra were acquired using a ZnSe ATR crystal-equipped Bruker Alpha FTIR spectrometer operated at 4 cm⁻¹ spectral resolution and 32 scans. Raman spectroscopy measurements were carried out using a Bruker Senterra Raman spectrometer equipped with a diode laser at 785 nm and 1 mW of laser power that focused on samples' surface using an Olympus long-working-distance MPlan semiapochromat objective lens (50×) for the 30s. The Raman spectrometer was equipped with an Andor iDus DU420A CCD detector operating in a deep-cool mode at -80 °C. To determine the SPAN's electrical conductivity in the form of a pellet, we used an LCR meter Agilent E4980A with 1 V of applied signal amplitude and 20 kHz – 100 kHz of working frequencies. The degree of sulfonation was determined by calculating the sulfur-to-nitrogen atomic ratio from the Energy Dispersive X-Ray Spectroscopy (EDXS) using an SEM JEOL-JSM-6510LV. Current density-voltage (*J-V*) measurements of DSSC were performed using a Keithley 2400 source meter under the illumination of a Newport ORIEL S013A solar simulator (AM 1.5 G, 100 mW cm⁻²). All characterizations were performed at an ambient temperature of 20 °C with less than 60% relative humidity.

Based on the *J-V* curve, we can obtain photovoltaic *FF* parameters using the following Eq. 1^[43]

$$FF = \frac{P_M}{J_{SC} \times V_{OC}} = \frac{J_M \times V_M}{J_{SC} \times V_{OC}} \quad (1)$$

J_{SC} is the short-circuit current density, V_{OC} is the open-circuit voltage, J_M is the current density at the maximum power, and V_M is the maximum power voltage. Fill Factor (*FF*) is how “square” the *J-V* curve is. Power conversion efficiency (*PCE*) can be calculated using the below formula (Eq. 2)

Table 1. Variation of sulfonation duration and ClSO_3H concentration used to synthesis SPAN in this study with its corresponding sample code.

No.	Sample code	Duration (h)	ClSO_3H concentration (% v/v)
1	SPAN 24 h	24	20
2	SPAN 48 h	48	20
3	SPAN 72 h	72	20
4	SPAN 5%	72	5
5	SPAN 10%	72	10
6	SPAN 20%	72	20
7	SPAN 30%	72	30
8	SPAN 40%	72	40

$$PCE = \frac{P_M}{P_{in}} \times 100\% \quad (2)$$

where P_{in} is the light power incident from the solar simulator. The photograph of solar simulator instrumental setup is shown in Figure S2a, while the schematic of the setup is depicted in Figure S2b. The DSSC prototype prepared in this study is also shown as the inset in Figure S2b.

3. Results and discussion

3.1. Synthesis of SPAN

SO₃ is a very reactive electrophilic sulfonating agent that reacts vigorously with any organic compound containing nucleophiles or electron donor groups. Sulfonation of organic compounds is a challenging task to perform and control due to its highly exothermic and rapid reaction, releasing approximately 380 kJ per kg of reacted

SO₃.^[44] Historically, the SO₃ reactivity problem has been approached by decreasing the reaction temperature, diluting, and complexing the SO₃ to reach a moderate reaction rate. Common diluting or complexing agents are commercially available, like dioxane (SO₃), ammonia (sulfamic acid), hydrochloric acid (chlorosulfuric acid or oleum), and dry air (air/SO₃ film sulfonation).^{[31]45-47} Controlling the ratio of SO₃ to the raw organic material is essential in achieving the quality of the desired product in any sulfonating agents. These processes also require heat management or reaction temperature control, maintaining the product quality from any undesired thermal degradations. Therefore, most sulfonation processes were carried out at low reaction temperatures, i.e., near 0 °C or below.

Chlorosulfuric acid (ClSO₃H) is widely used to produce alcohol sulfates, alcohol ether sulfates, dyes, and dye intermediates.^[47] ClSO₃H is a rapid, efficient, and stoichiometric reagent to perform any sulfonation reactions grace of the attached chloro- group, an excellent leaving group.^[48-50] However, it will be immediately hydrolyzed and inactive in the presence of water molecules, i.e., moisture. To avoid this, we usually add a nonpolar solvent, like chloroform (CHCl₃), to prevent the moisture from incorporating into the ClSO₃H solution. However, we used a unique approach in this study, where the concentrated sulfuric acid (H₂SO₄) was introduced to dissolve ClSO₃H, then the solution acted as the sulfonating agent. This new type of sulfonating agent provides several advantages compared to the conventional CHCl₃ system. First, PANI readily dissolves in this very acidic system because the

concentrated sulfuric acid can protonate PANI almost completely, forming a soluble protonated PANI that is easier to be sulfonated. Second, a very acidic condition makes the aromatic rings in PANI relatively more basic, causing the sulfonation reaction to be carried out more selectively. Third, the concentrated sulfuric acid is very hygroscopic, consuming any moisture immediately, maintaining the diluted chlorosulfuric acid to be always reactive. Fourth, the sulfonation using this type of sulfonating agent can be carried out at room temperature because PANI is an unreactive and stable aromatic system that cannot be substituted easily.

3.2. Molecular structure investigation

Figure 1a presents the sulfonation process of PANI to obtain SPAN in this study. FTIR measurements were performed to characterize synthesized PANI and SPAN (Figure 1b), revealing their functional groups. A broad absorption band typical of the conducting form of PANI is observed at wavenumber above 1600 cm⁻¹. The main characteristic absorption peaks of PANI and SPAN are associated with the stretching of C-H out-plane bending vibration (804 cm⁻¹), N=Q=N, Q=N⁺-B, and B-NH⁺-B (1130-1150 cm⁻¹), C~N.⁺ stretching vibrations in the polaronic structure (1214-1250 cm⁻¹), C-N (1298 cm⁻¹), and C=C from benzenoid rings (1500 cm⁻¹) and quinonoid rings (1570 cm⁻¹).^[40,51,52] These peaks relatively shifted to the lower wavenumber for SPAN. The ~ sign denotes the bond intermediate between the single and double bonds. Four new peaks occurred in SPAN, which is corresponded to the symmetric and asymmetric stretching of S=O (1064 and 1011 cm⁻¹), which overlap with a broad, intense absorption extending from 850 to 1100 cm⁻¹, stretching of S-O (700 cm⁻¹), and C-S (598 cm⁻¹).^[15,40,53,54]

Figure 1c shows the Raman spectra of PANI and SPAN, which confirms the FTIR results. These two molecules' main characteristic bands are associated with the peak observed at 1619 and 1585 cm⁻¹ representing C=C stretching vibrations in benzenoid and quinonoid rings. The peak with a maximum at 1503 cm⁻¹ corresponds to the N-H deformation associated with the semiquinonoid structures. The band at 1354 cm⁻¹ provides information on the C~N.⁺ vibrations of delocalized polaronic structures. The other peaks are the stretching vibration of C-H (1167 cm⁻¹), bending vibration of C-N-C (818 cm⁻¹), and C-N=C (716 cm⁻¹), in-plane deformation of benzenoid rings (586 cm⁻¹) and amine groups (522 cm⁻¹).^[35] Two new features occurred in the Raman spectra of SPAN, which are corresponded to the sulfonic group represented by

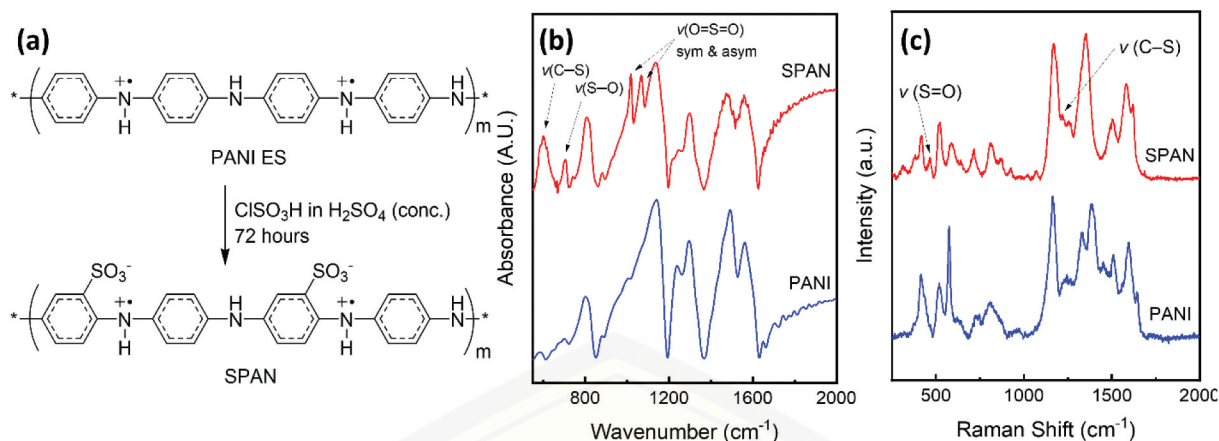


Figure 1. (a) Schematic representation of sulfonation reaction of PANI ES using chlorosulfuric acid. (b) FTIR and (c) Raman spectra of synthesized PANI and SPAN, respectively. New peaks are formed after the sulfonation process, corresponding to the sulfonic group's characteristic vibrational mode ($-\text{SO}_3\text{H}$).

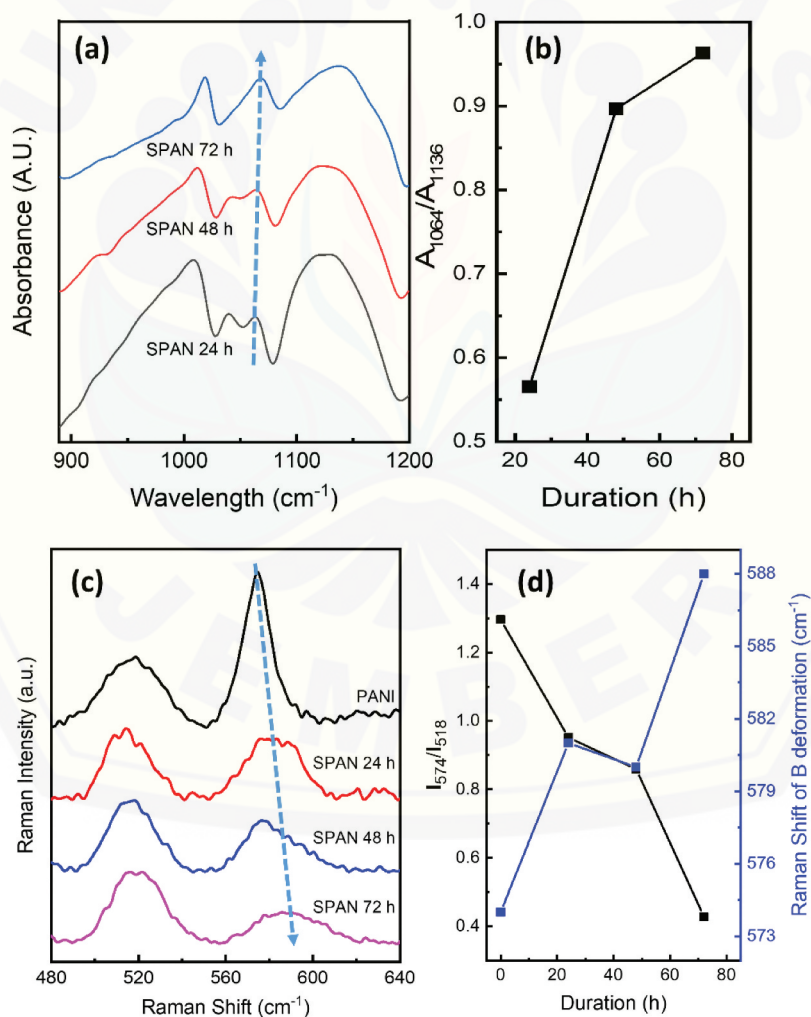


Figure 2. (a) The evolution of FTIR absorption peak at 1064 cm^{-1} , corresponding to the symmetric stretching vibration of $\text{S}=\text{O}$, against the sulfonation duration. (b) The relationship between A_{1064}/A_{1136} with the sulfonation duration. (c) Raman spectra show the evolution of the in-plane deformation of benzenoid rings. (d) I_{574}/I_{518} and Raman shift of benzenoid ring in-plane deformation with the sulfonation duration.

stretching vibration of S=O (peak at 467 cm^{-1}) and C(aryl)-S (shoulder at 1215 cm^{-1}). All results indicate that the sulfonation process has been successfully carried out.

3.3. Variation of duration

We investigate the effect of PANI's sulfonation duration by using a solution of 20% (v/v) ClSO_3H in concentrated H_2SO_4 as a sulfonating agent. We observed the sulfonation process in 24, 48, and 72 h. Figure 2a shows the peak evolution at 1064 cm^{-1} of FTIR spectra, which corresponds to the symmetric stretching vibration of S=O. This peak is not fully formed at SPAN 24 h and 48 h indicating that the sulfonic group does not completely attach to the PANI chain. However, this peak was observed clearly and more intense in SPAN 72 h than others, as presented in Figure 2b., showing the ratio between the absorbance of peaks observed at 1064 cm^{-1} and 1136 cm^{-1} (A_{1064}/A_{1136}) with the sulfonation duration. The peak at 1136 cm^{-1} corresponds to the C-H bending and stretching (18b),^[51] which remains unchanged during the sulfonation reaction. Figure 2c shows the peak evolution at 574 cm^{-1} in Raman spectra, corresponding to the benzenoid rings' in-plane deformation. This peak intensity decreases with sulfonation duration and even becomes lower than the peak at 518 cm^{-1} , associating with the amine groups.^[55] Figure 2d presents the relationship curve between the Raman intensity ratio of peaks observed at 574 cm^{-1} to 518 cm^{-1} (I_{574}/I_{518}) and sulfonation duration. The

decrease of I_{574}/I_{518} is due to the increase of the sulfonic group number attached to the PANI chain affecting the benzenoid rings' in-plane deformation. As the duration of sulfonation increases, the number of the sulfonic group attached to the PANI chain increases, causing the benzenoid ring's deformation to become more rigid. It also causes the peak at 574 cm^{-1} to shift to higher-value or blue-shifted around $6\text{--}15\text{ cm}^{-1}$ (Figure 2d). Therefore, we can conclude that the sulfonic group has been successfully introduced into the PANI chain after 72 h.

The presence of the sulfonic group in the polymer backbone also affects the electrical conductivity of SPAN. A sulfonic group is an electron-withdrawing group in an aromatic system that reduces the system's electron density and decreases the sample's conductivity value. Figure 3a shows the conductivity profile of the synthesized SPAN as a function of frequency. We noted that the SPAN's electrical conductivity decreases nearly ten times than PANI as we introduce the sulfonic group (Figure 3b). This behavior is observed in a SPAN of 48 h. The origin of the lower conductivity can be attributed to the decreased interchain diffusion of the charge carriers. The typical charge carriers' interchain diffusion is induced by the increase of the polymer chains separation due to the side groups' presence and also due to the lower crystallographic order (hence the reduced coherence) among the chains.^[56] However, SPAN's conductivity increases after 72 h of sulfonation. The higher conductivity after 72 h is due to the increase in the attached sulfonic groups to the PANI chain, leading to

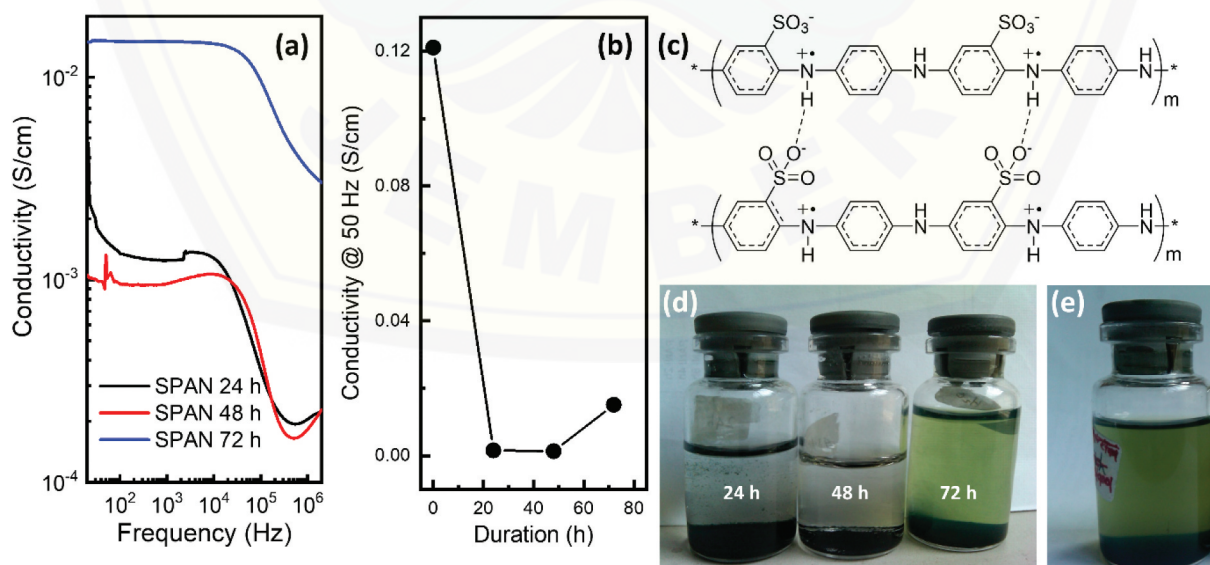


Figure 3. (a) Frequency response profile and (b) electrical conductivity value at 50 Hz of synthesized SPAN with various sulfonation duration. (c) The intermolecular interaction between SPAN chains through hydrogen bonding. (d) The solubility of synthesized SPAN with different sulfonation duration in water. (e) SPAN 72 h also demonstrates good solubility in ethanol.

the intermolecular interactions among SPAN chains (Figure 3c). This type of interchain interaction may play an essential role in increasing the three-dimensionality of the charge and spin motion, increasing conductivity.^[35]

Figure 3d shows the solubility of synthesized SPAN in water (1 mg mL^{-1}) with various sulfonation duration. SPAN starts to dissolve after 72 h, due to the sulfonic group being completely attached to PANI chains. The sulfonic group is vital in increasing SPAN's polarity, causing it to be soluble in some nontoxic polar solvents. Besides in water, the synthesized SPAN is also soluble in ethanol, as shown in Figure 3e.

3.4. Variation of concentration

We also investigate the effect of different concentrations of ClSO_3H used. Figure 4a shows the peak evolution at 1064 cm^{-1} in the SPAN FTIR spectra synthesized using ClSO_3H with a concentration from 5 to 40%. This peak represents the sulfonic group attached to the polymer chain. This peak intensity increases significantly until the ClSO_3H concentration of 20% and remains relatively constant at higher ClSO_3H concentration. Similar behavior is also observed in Raman spectra for the evolution of peak intensity at 467 cm^{-1} (I_{467}), representing the S=O stretching mode (Figure 4b). This peak intensity also increases then saturates with ClSO_3

H concentration, supporting the FTIR results. Figure 4c presents the relationship curve between stretching vibration of S=O represented by A_{1064}/A_{1136} obtained by FTIR and I_{467} obtained by Raman as a function of ClSO_3H concentration. This situation indicates that the system saturates when using ClSO_3H concentration higher than 20%, which means that no matter if we add more ClSO_3H , the number of sulfonic groups attached to PANI is still the same. The different ClSO_3H concentration used in this study affects the solubility of SPAN. Figure 4d shows the solubility of 1 mg mL^{-1} of SPAN in water, and it increases as the ClSO_3H concentration increases. It is observed that SPAN 20 to 40% are soluble in water while the others are not. SPAN's solubility depends on the amount of the sulfonic group attached to the polymer backbone, which can be determined by the peak intensity of the S=O group's stretching vibration in FTIR spectra. Therefore, we can conclude that the solubility results are in good agreement with FTIR and Raman results (Figure 4c).

The electrical conductivity of SPAN is also affected by the different ClSO_3H concentrations used. The green protonated SPAN has conductivity on a semiconductor level. This value is many orders of magnitude higher than common polymer ($10^{-9} \text{ S cm}^{-1}$) but lower than typical metals (10^4 S cm^{-1}). Figure 5a shows the conductivity profile of the SPAN with various ClSO_3H concentrations. The

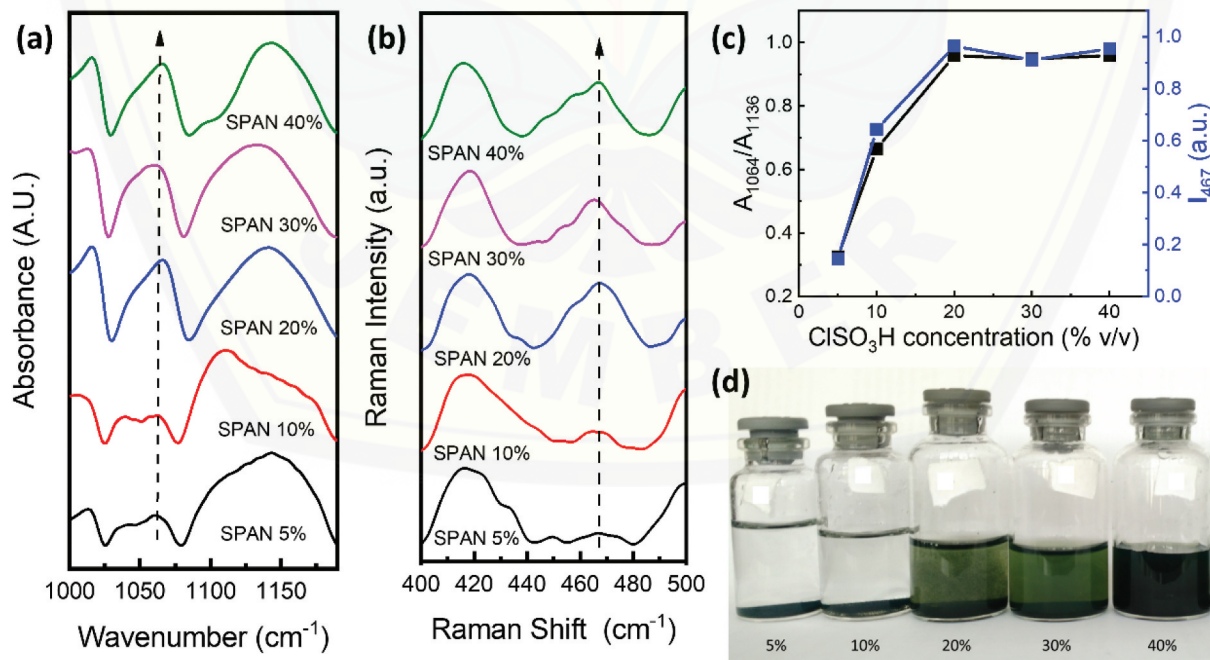


Figure 4. The evolution of (a) FTIR peak absorbance at 1064 cm^{-1} and (b) Raman intensity at 467 cm^{-1} as a function of ClSO_3H concentration. (c) Relationship curve between stretching vibration of S=O represented by A_{1064}/A_{1136} obtained by FTIR and I_{467} obtained by Raman as a function of ClSO_3H concentration. (d) The solubility of synthesized SPAN using different ClSO_3H concentrations in water.

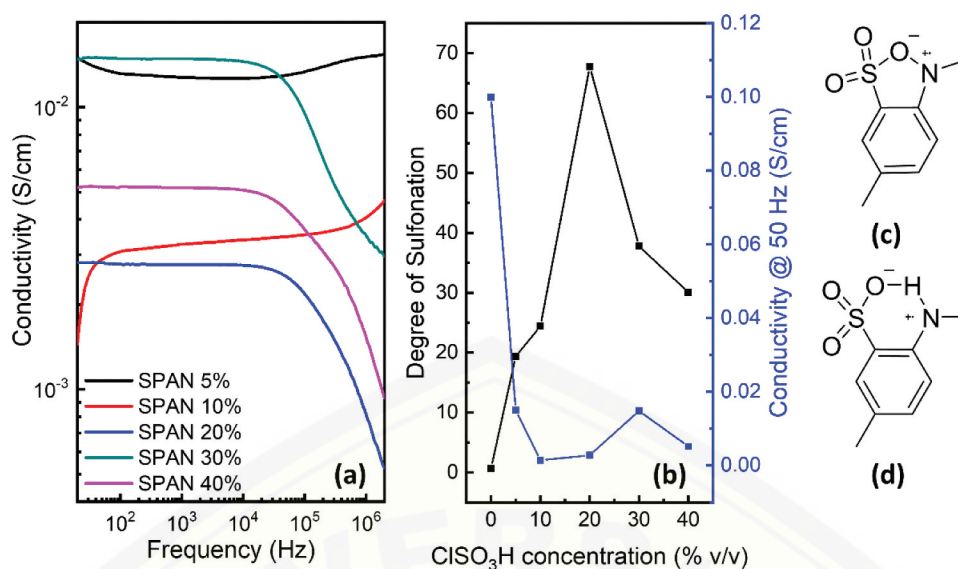


Figure 5. (a) Frequency response profile of SPAN's conductivity with corresponding ClSO₃H concentration. (b) The degree of sulfonation and conductivity of SPAN at 50 Hz as a function of ClSO₃H concentration. Two possible intramolecular interactions between the sulfonic group and the PANI chain. The cationic nitrogen radical or the hydrogen atom from the PANI chain can interact with a sulfonic group to form a (c) five- or (d) six-member ring.

conductivity graph indicates three regions: dispersion in the low-frequency area, an intermediate plateau, and conductivity dispersion at the high-frequency region. Thus, conductivity is independent of frequency in the low-frequency region (like a straight line), generally known as the hopping frequency. The increasing value of SPAN 5 and 10% conductivity with frequency rise is due to the disordering of cations between neighboring sites, the presence of space charge, and the formation of excess charge carriers (polaron and bipolaron).^[57] On the other hand, this phenomenon is not observed in SPAN 20, 30, and 40%, which have the opposite behavior.

We can determine SPAN's average sulfonation degree by comparing the sulfur and nitrogen atom percentage from the EDXS analysis results (Figure 5b). Sulfur and nitrogen atoms represent the sulfonic group and polyaniline itself, respectively. The maximum conductivity was obtained at SPAN 5% due to the least number of the sulfonic group attached to PANI. It decreases at 10% and then increases, reaching the second maximum at 30% before it decreases. The fluctuation conductivity is due to the strong intramolecular interactions between sulfonic group and cationic radical nitrogen atoms or hydrogen bonding through space to form five or six-member rings, which are energetically favorable configurations (see Figure 5 c and d). Such molecular arrangements can localize the positive charge around the nitrogen atoms.^[35]

3.5. Counter electrode properties

Figure 6a shows the morphology of SPAN 30%, indicating that SPAN's surface is porous and has an agglomerated granules structure ranging from 100 to 500 nm. Granules are formed by the agglomeration of polymers interacting with each other using hydrogen bonding.^[58] We can obtain another structure or morphology of SPAN by using other synthesis methods.^[21] Figure 6b shows the surface morphology of the fabricated graphite counter electrode using the screen print method. It has plate-like morphology composed of several layers. Figure 6c shows the surface morphology of PANI:graphite blend counter electrode where PANI's particles have covered the graphite resembling a group of Islands. SPAN:graphite blend counter electrode yields a more fine surface morphology than PANI (Figure 6d), indicating that SPAN and graphite are well blended and covered the graphite. We also investigate the interaction between SPAN:graphite blend counter electrode and electrolyte solution using Raman spectroscopy (Figure 7). Some changes are observed after adding electrolyte solution to the counter electrode. Raman intensity at 1506 and 1619 cm⁻¹, corresponding to the N-H deformation associated with the semiquinoid structures and C=C stretching vibrations in benzenoid, respectively, increased with electrolyte solution addition. Due to SPAN's oxidative doping reaction by the electrolyte, intramolecular redox reaction occurs in the quinonoid unit. It leads to the semiquinone dicationic

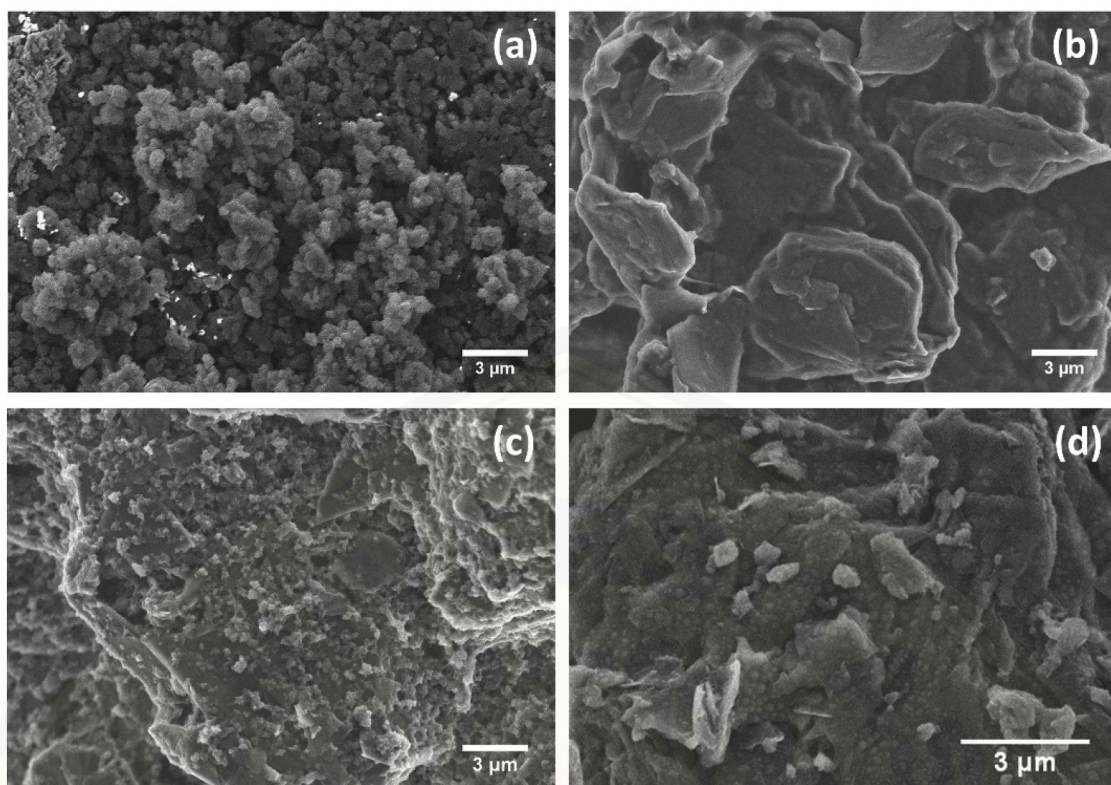


Figure 6. SEM images of (a) SPAN 30%, fabricated counter electrode using (b) pure graphite, (c) PANI:graphite blend and (d) SPAN:graphite blend.

radical formation followed by the charge delocalization. Finally, the polysemiquinoid structure was formed.^[59] The graphite E_{2g2} mode in Raman spectra is blue-shifted

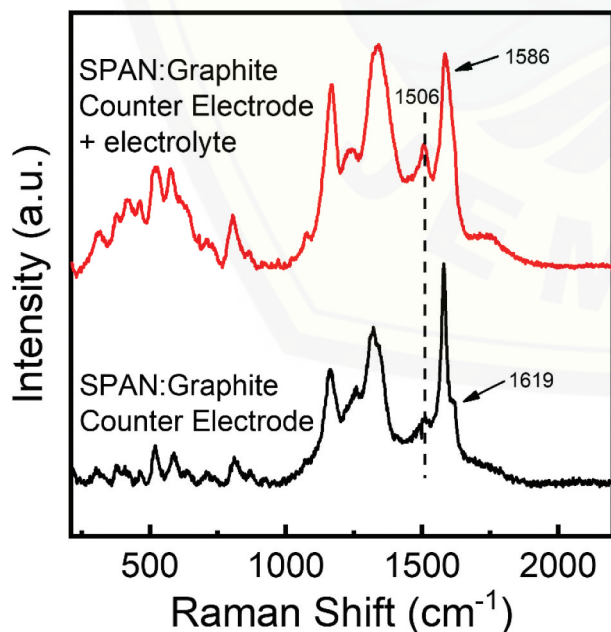


Figure 7. Raman spectra of fabricated SPAN:graphite counter electrode before and after electrolyte addition for SPAN 30%.

(1586 cm^{-1}) by about 6 cm^{-1} compared to that found in Raman spectra of counter electrode only (1580 cm^{-1}). The blue-shifted Raman mode at around 1580 cm^{-1} is due to the I_2 intercalated graphite species in SPAN:graphite blend counter electrode. We also investigated the structure of SPAN 30%:graphite blend counter electrode using XRD, however the XRD pattern is dominated by the graphite peaks overcoming the SPAN structural features despite of their considerable concentration, i.e., 25% (w/w) (please see Figure S3).

3.6. Photovoltaic performance

We made a DSSC prototype using SPAN 30% as an additive in the graphite-based counter electrode (Figure 8a) regarding the structural and electronic properties characterizations. Please see the inset in Figure S2b for the photograph of the DSSC prototype. We varied the mass percentage of SPAN 30% against graphite to obtain the optimum composition. The current density-voltage (J - V) curve of DSSC (Figure 8b) shows that the SPAN 30% acts as an additive in the counter electrode, which increases the efficiency performance of DSSC with respect to the graphite counter electrode. The DSSC performance improved due to its porous morphology with

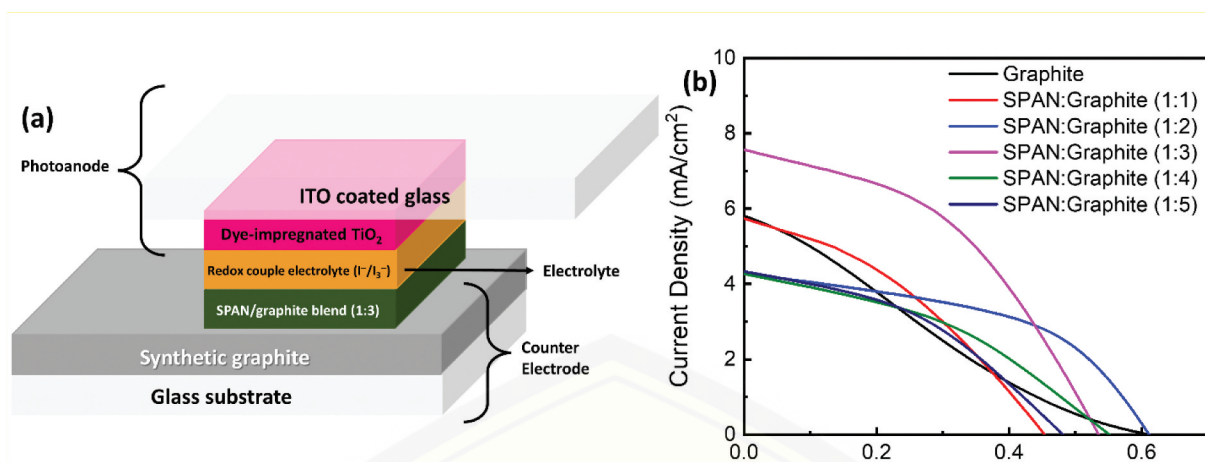


Figure 8. (a) Schematic illustration of fabricated DSSC. (b) Current density-voltage (J-V) curve of DSSC using SPAN:graphite blend as a counter electrode with various mass ratio compositions.

Table 2. Photovoltaic parameters of fabricated DSSC using SPAN:graphite counter electrodes with various compositions compared to commercial platinum (Pt) counter electrode.

No.	Counter Electrode	J_{sc} (mA cm^{-2})	V_{oc} (V)	FF	PCE (%)	Average PCE (%)
1	Graphite	5.51	0.61	0.219	0.87	0.86 ± 0.01
2	SPAN:Graphite (1:1)	5.73	0.46	0.354	1.05	1.04 ± 0.01
3	SPAN:Graphite (1:2)	4.27	0.61	0.486	1.42	1.40 ± 0.02
4	SPAN:Graphite (1:3)	7.56	0.53	0.432	1.95	1.93 ± 0.02
5	SPAN:Graphite (1:4)	4.27	0.56	0.377	1.01	1.00 ± 0.01
6	SPAN:Graphite (1:5)	4.33	0.48	0.395	0.93	0.92 ± 0.01
7	PANI:Graphite (1:3) ^a	5.05 ^a	0.60 ^a	0.447 ^a	1.50 ^a	-
8	Pt ^b	11.00 ^b	0.71 ^b	0.741 ^b	5.78 ^b	-

^aSunarya et al.^[27]

^bKusumawati et al.^[61]

a large surface area, providing more places to conduct the electrolyte redox cycle. Moreover, SPAN has a better electrocatalytic activity (noted by higher FF values) than graphite, which can be quantified by the small R_{CT} (Charge Transfer Resistance) value for the I_3^-/I^- reduction process.^[60]

Table 2 shows that the counter electrode with the mass ratio of SPAN to graphite 1:3 produces the highest efficiency (PCE) of 1.95% and photocurrent density (J_{sc}) of 7.56 mA cm^{-2} . We can conclude that this is the optimum composition, attaining an outstanding balance between electrical conductivity provided by graphite and electrocatalytic activity provided by SPAN. Here, SPAN serves as a better electrocatalyst in the blend, providing a synergy effect between conducting polymer and graphite in the counter

electrode, even with respect to PANI. SPAN:Graphite (1:3) blend counter electrode excels PANI:Graphite (1:3) blend counter electrode in both PCE and J_{sc} (see Table 2). However, this efficiency value is still about three times smaller than the efficiency of DSSC using a Pt-based counter electrode. Nevertheless, our result is still acceptable concerning the manual DSSC fabrication method carried out in this study (i.e., screen printing, liquid immersion).

4. Conclusion

We have synthesized a nontoxic polar-solvent-soluble sulfonated polyaniline (SPAN) having metallic properties with a conductivity of $1.48 \times 10^{-2} \text{ S cm}^{-1}$. Electrical conductivity measurements revealed that SPAN has the conductivity value within the semiconductor range (10^{-2} to $10^{-3} \text{ S cm}^{-1}$). SPAN was directly prepared from polyaniline emeraldine salt (PANI ES) by a simple moistureproof sulfonation method at room temperature. PANI ES was dissolved in a sulfonating agent, a chlorosulfuric acid solution (ClSO_3H), in concentrated sulfuric acid (H_2SO_4) with various concentrations. This study's optimum condition to synthesize SPAN is a 30% (v/v) ClSO_3H in concentrated H_2SO_4 for 72 h of sulfonation. The number of sulfonic groups ($-\text{SO}_3\text{H}$) attached to polymer chains determines the SPAN's solubility, as shown by the S=O vibrational stretching mode at 1064 cm^{-1} in FTIR spectra and 467 cm^{-1} in Raman spectra. The synthesized SPAN has a porous morphology that can increase the electrocatalytic activity of the counter electrode. Therefore, SPAN

can be used as an additive in the graphite-based counter electrode for DSSC application marked by the increase of FF , J_{sc} , and PCE value. The photovoltaic performance increases due to a perfect combination between the high-conductive graphite and the electrocatalytic-active SPAN. The future studies should be further addressed on the issues of the SPAN interactions with graphite facilitating electrocatalytic activity through the charge transfer between them, understanding the effect of SPAN on the photoelectrical up conversion processes, and designing alternative fabrication method of SPAN: graphite composite to enhance the charge carrier transport efficiency and to improve the stability of the PV cells.

Acknowledgments

This work was financially funded by ITB Research Grant 2020 through ITB Research and Innovation Program 2020 (No. 2G/I1.C01/PL/2020). The authors would like to thank Dr. Yessi Permana and Ms. Eunike Kartika Salduna (Department of Chemistry, Institut Teknologi Bandung – Indonesia) for providing XRD characterization depicted in Figure S3.

Disclosure statement

No potential conflict of interest was reported by the author(s).

Funding

This work was supported by the Lembaga Penelitian dan Pengabdian Kepada Masyarakat [ITB Research and Innovation No. 2G/I1.C01/PL/2020].

Notes on contributors

M. Reza was born in Indonesia. He received a bachelor's degree in Chemistry from Institut Teknologi Bandung, Bandung, Indonesia in 2014 under the supervision of Dr. Veinardi Suendo. He received a master's degree in Matériaux et Technologies Associées from Université d'Aix-Marseille, Marseille, France, in 2015 and also from Institut Teknologi Bandung, Bandung, Indonesia in 2016. He received a doctor's degree in Institut Teknologi Bandung in 2021 with focusing on conducting polymer for DSSC applications and development. He is currently working as lecturer in Chemistry Department, Universitas Jember.

Fauziah Nurfalih was born in Indonesia. She completed her bachelor's degree in Chemistry Education at Universitas Pendidikan Indonesia, Bandung, Indonesia in 2012, under the supervision Dr. Kurnia M.Si. She received a master's degree under the supervision of Dr. Veinardi Suendo in

chemistry from Institut Teknologi Bandung, Bandung, Indonesia in 2016. Her research is focused on conducting polymer for DSSC applications and development.

Triannisa Rahmawati was born in Indonesia. He received a bachelor's degree in Chemistry Education from Department of Chemistry Education, Universitas Pendidikan Indonesia, Bandung, Indonesia in 2014. She received a master's degree in Chemistry Department (physical chemistry) from Institut Teknologi Bandung, Bandung, Indonesia in 2018 under the supervision of Dr. Veinardi Suendo. Her research interest includes graphene, nanofiber, membrane, also chemistry education, specifically in chemistry evaluation and assessment. She is currently work as lecturer in Department of Chemistry Education, Universitas Pendidikan Indonesia.

Phutri Milana was born in Indonesia. She received the bachelor's degree in Chemistry Education from Universitas Negeri Padang, Padang, Indonesia, in 2010, under the supervision of Syukri S., S. Si, M.Pd. and Dra. Bayharti, M.Sc. She received the master's degree in 2012 from the Division of Organic Chemistry, and the doctor's degree in 2019 from the Division of Inorganic and Physical Chemistry, both division in Department of Chemistry, Institut Teknologi Bandung, Bandung, Indonesia. Research interests in the field of chemistry education are problem-based learning to develop the skill of learners and research interests in the field of chemistry are synthesis and characterizations of organic dyes for Dye-Sensitized Solar Cells (DSSC) applications.

A. N. Amalina was born in Balikpapan, Indonesia. She received Bachelor of Science in chemistry from Institut Teknologi Bandung in 2018. She received Master of Science in chemistry (physical chemistry) from Institut Teknologi Bandung in 2021. Both the thesis in bachelor's and master's degree are under supervision of Dr. Veinardi Suendo. Research interest are in synthesis process and the properties of conductive polymer of polyaniline for Dye-Sensitized Solar Cells (DSSC) applications, and the adsorption process of Titania Oxide in DSSC.

R.R. Sunarya was born in Bandung, Indonesia. She received the bachelor's degree in Chemistry from Universitas Pendidikan Indonesia, Bandung, Indonesia, in 2004. The master's degree from Department of Chemistry Teaching, Institut Teknologi Bandung, Bandung, Indonesia, in 2009, under the supervision of Prof. Dr. Ismunandar. And The doctor's degree from Department of Chemistry, Division of Inorganic and Physical Chemistry, Institut Teknologi Bandung, Bandung, Indonesia, in 2020, under the supervision of Dr. Veinardi Suendo. She is working as Assistant Professor at Universitas Islam Negeri (UIN) Sunan Gunung Djati, Bandung, Indonesia since 2009. Her research interest include synthesis and characterize carbon-based materials and conductive polymer for Dye-Sensitized Solar Cells (DSSC) applications.

F. V. Steky completed his bachelor's and master's degree in 2018 and 2021, respectively, in chemistry at Institut Teknologi Bandung, Indonesia under the supervision of Dr. Veinardi Suendo. He was recruited as an academic assistant in the Department of Chemistry, Institut Teknologi Bandung for 2019-2021. Research interests in the development of

nanostructured oxide materials based on titania. These cover their optoelectronic properties, synthesis route, chemical modification, and molecular spectroscopic.

V. Suendo graduated in Chemistry from Institut Teknologi Bandung, Indonesia in 1998. He was recruited as an assistant in the Department of Chemistry at the Institut Teknologi Bandung in 1999. He obtained his M.Eng. from the Department of Organic and Polymeric Materials, Tokyo Institute of Technology, Japan in 2001. In the same year, he moved to France to pursue his Ph.D. at the Ecole Polytechnique, Palaiseau in the department of physics. In 2005, he completed his Ph.D. at Laboratoire de Physique des Interfaces et Couches Minces, Ecole Polytechnique under the supervision of Professor Pere Roca i Cabarrocas. After returned to Institut Teknologi Bandung in 2006, he commenced his new academic career in the Department of Chemistry, where he was promoted to Lecturer in 2008. In 2013, he started a new page as an independent scientist when he was promoted to Associate Professor. Research interests include the development of new organic electronics materials based on porphyrin molecules, anthocyanins, nano carbons, and polyaniline. These cover their optoelectronic properties, synthesis route, chemical modification, wet-process device fabrications, and molecular spectroscopies.

ORCID

Muhammad Reza  <http://orcid.org/0000-0003-0001-5918>
 Phutri Milana  <http://orcid.org/0000-0003-0931-0884>
 Auliya Nur Amalina  <http://orcid.org/0000-0003-4300-7459>
 Risa Rahmawati Sunarya  <http://orcid.org/0000-0003-4425-2931>
 Fry Voni Steky  <http://orcid.org/0000-0003-0512-3985>
 Veinardi Suendo  <http://orcid.org/0000-0002-3402-433X>

References

- [1] O'Regan, B.; Grätzel, M. A. A Low-cost, High-efficiency Solar Cell Based on Dye-sensitized Colloidal TiO₂ Films. *Nature*. 1991, 353(6346), 737–740. DOI: 10.1038/353737a0.
- [2] Nazeeruddin, M. K.; Kay, A.; Humpbry-Baker, R.; Miiller, E.; Liska, P.; Vlachopoulos, N.; Gratzel, M. Conversion of Light to Electricity by Cis-XzBis(2,2'-Bipyridyl-4,4'-Dicarboxylate)Ruthenium(II) Charge-Transfer Sensitizers (X = Cl-, Br-, I-, CN-, and SCN-) on Nanocrystalline TiO₂ Electrodes. *J. Am. Chem. Soc.* 1993, 115, 6382–6390. DOI: 10.1021/ja00067a063.
- [3] Li, Q.; Tang, Q.; Lin, L.; Chen, X.; Chen, H.; Chu, L.; Xu, H.; Li, M.; Qin, Y.; He, B. A Simple Approach of Enhancing Photovoltaic Performances of Quasi-Solid-State Dye-Sensitized Solar Cells by Integrating Conducting Polyaniline into Electrical Insulating Gel Electrolyte. *J. Power Sources*. 2014, 245, 468–474. DOI: 10.1016/j.jpowsour.2013.07.006.
- [4] He, B.; Tang, Q.; Luo, J.; Li, Q.; Chen, X.; Cai, H. Rapid Charge-Transfer in Polypyrrole-Single Wall Carbon Nanotube Complex Counter Electrodes: Improved Photovoltaic Performances of Dye-Sensitized Solar Cells. *J. Power Sources*. 2014, 256, 170–177. DOI: 10.1016/j.jpowsour.2014.01.072.
- [5] Grätzel, M. Dye-Sensitized Solar Cells. *J. Photochem. Photobiol. C Photochem. Rev.* 2003, 4(2), 145–153. DOI: 10.1016/S1389-5567(03)00026-1.
- [6] Wu, J.; Lan, Z.; Lin, J.; Huang, M.; Huang, Y.; Fan, L.; Luo, G. Electrolytes in Dye-Sensitized Solar Cells. *Chem. Rev.* 2015, 115(5), 2136–2173. DOI: 10.1021/cr400675m.
- [7] Hagfeldt, A.; Grätzel, M. Molecular Photovoltaics. *Acc. Chem. Res.* 2000, 33(5), 269–277. DOI: 10.1021/ar980112j.
- [8] Bach, U.; Lupo, D.; Comte, P.; Moser, J. E.; Weissörtel, F.; Salbeck, J.; Spreitzer, H.; Grätzel, M. Solid-State Dye-Sensitized Mesoporous TiO₂ Solar Cells with High Photon-to-Electron Conversion Efficiencies. *Nature*. 1998, 395(6702), 583–585. DOI: 10.1038/26936.
- [9] Chiba, Y.; Islam, A.; Watanabe, Y.; Komiya, R.; Koide, N.; Han, L. Dye-Sensitized Solar Cells with Conversion Efficiency of 11.1%. *Jpn. J. Appl. Phys.* 2006, 45(No. 25), L638–L640. DOI: 10.1143/JJAP.45.L638.
- [10] Luo, Y.; Li, D.; Meng, Q. Towards Optimization of Materials for Dye-Sensitized Solar Cells. *Adv. Mater.* 2009, 21(45), 4647–4651. DOI: 10.1002/adma.200901078.
- [11] Papageorgiou, N.; Maier, W. F.; Grätzel, M. An Iodine/Triiodide Reduction Electrocatalyst for Aqueous and Organic Media. *J. Electrochem. Soc.* 1997, 144(3), 876–884. DOI: 10.1149/1.1837502.
- [12] Kim, -S.-S.; Nah, Y.-C.; Noh, -Y.-Y.; Jo, J.; Kim, D.-Y. Electrodeposited Pt for Cost-Efficient and Flexible Dye-Sensitized Solar Cells. *Electrochim. Acta*. 2006, 51(18), 3814–3819. DOI: 10.1016/j.electacta.2005.10.047.
- [13] Olsen, E.; Hagen, G., and Lindquist, S. E. Dissolution of Platinum in Methoxy Propionitrile Containing Li/I. *Sol. Energy Mater.* 2000, 63(3), 267–273. DOI:10.1016/S0927-0248(00)00033-7.
- [14] Hino, T.; Ogawa, Y.; Kuramoto, N. Preparation of Functionalized and Non-Functionalized Fullerene Thin Films on ITO Glasses and the Application to a Counter Electrode in a Dye-Sensitized Solar Cell. *Carbon*. 2006, 44(5), 880–887. DOI: 10.1016/j.carbon.2005.10.027.
- [15] Chen, J.; Li, K.; Luo, Y.; Guo, X.; Li, D.; Deng, M.; Huang, S.; Meng, Q. A Flexible Carbon Counter Electrode for Dye-Sensitized Solar Cells. *Carbon*. 2009, 47(11), 2704–2708. DOI: 10.1016/j.carbon.2009.05.028.
- [16] Murakami, T. N.; Ito, S.; Wang, Q.; Nazeeruddin, M. K.; Bessho, T.; Cesar, I.; Liska, P.; Humphry-Baker, R.; Comte, P.; Péchy, P., et al. Highly Efficient Dye-Sensitized Solar Cells Based on Carbon Black Counter Electrodes. *J. Electrochem. Soc.* 2006, 153(12), A2255. DOI: 10.1149/1.2358087.
- [17] Kay, A.; Grätzel, M. Low Cost Photovoltaic Modules Based on Dye Sensitized Nanocrystalline Titanium Dioxide and Carbon Powder. *Sol. Energy Mater. Sol. Cells*. 1996, 44(1), 99–117. DOI: 10.1016/0927-0248(96)00063-3.

- [18] Papageorgiou, N.; Liska, P.; Kay, A.; Grätzel, M. Mediator Transport in Multilayer Nanocrystalline Photoelectrochemical Cell Configurations. *J. Electrochem. Soc.* **1999**, *146*(3), 898–907. DOI: [10.1149/1.1391698](https://doi.org/10.1149/1.1391698).
- [19] Saito, Y.; Kubo, W.; Kitamura, T.; Wada, Y.; Yanagida, S. I-/I³⁻ Redox Reaction Behavior on Poly(3,4-Ethylenedioxythiophene) Counter Electrode in Dye-Sensitized Solar Cells. *J. Photochem. Photobiol. Chem.* **2004**, *164*(1–3), 153–157. DOI: [10.1016/j.jphotochem.2003.11.017](https://doi.org/10.1016/j.jphotochem.2003.11.017).
- [20] Wei, T. C.; Wan, C. C.; Wang, Y. Y. Poly(N-Vinyl-2-Pyrrolidone)-Capped Platinum Nanoclusters on Indium-Tin Oxide Glass as Counterelectrode for Dye-Sensitized Solar Cells. *Appl. Phys. Lett.* **2006**, *88*(10), 103122. DOI: [10.1063/1.2186069](https://doi.org/10.1063/1.2186069).
- [21] Utami, A. N.; Reza, M.; Benu, D. P.; Fatya, A. I.; Yuliarto, B.; Suendo, V. Reverse Micelle Facilitated Synthesis of Nanostructured Polyaniline as the Counter Electrode Materials in Dye-Sensitized Solar Cells. *Polym.-Plast. Technol. Mater.* **2020**, *59*(12), 1350–1358. DOI: [10.1080/25740881.2020.1738477](https://doi.org/10.1080/25740881.2020.1738477).
- [22] MacDiarmid, A. G. ^aSynthetic Metals^o: A Novel Role for Organic Polymers (Nobel Lecture)*. *Angew. Chem. Int. Ed.* **2001**, *40*(14), 2581–2590. doi:10.1002/1521-3773(20010716)40:14<2581::AID-ANIE2581>3.0.CO;2-2.
- [23] Kang, E. Polyaniline: A Polymer with Many Interesting Intrinsic Redox States. *Prog. Polym. Sci.* **1998**, *23*(2), 277–324. DOI: [10.1016/S0079-6700\(97\)00030-0](https://doi.org/10.1016/S0079-6700(97)00030-0).
- [24] Suendo, V.; Lau, Y.; Hidayat, F.; Reza, M.; Qadafi, A.; Rochliadi, A. Effect of Face-to-Face and Side-to-Side Interchain Interactions on the Electron Transport in Emeraldine Salt Polyaniline. *Phys. Chem. Chem. Phys.* **2021**, *23*(12), 7190–7199. DOI: [10.1039/D0CP06194H](https://doi.org/10.1039/D0CP06194H).
- [25] Amalina, A. N.; Suendo, V.; Reza, M.; Milana, P.; Sunarya, R. R.; Adhika, D. R.; Tanuwijaya, V. V. Preparation of Polyaniline Emeraldine Salt for Conducting-Polymer-Activated Counter Electrode in Dye Sensitized Solar Cell (DSSC) Using Rapid-Mixing Polymerization at Various Temperature. *Bull. Chem. React. Eng. Catal.* **2019**, *14*(3), 521. DOI: [10.9767/bcrec.14.3.3854.521-528](https://doi.org/10.9767/bcrec.14.3.3854.521-528).
- [26] Fatya, A. I.; Reza, M.; Sunarya, R. R.; Suendo, V. Synthesis of Polyaniline/Electrochemically Exfoliated Graphene Composite as Counter-Electrode in Dye-Sensitized Solar Cell. *Polym.-Plast. Technol. Mater.* **2020**, *59*(12), 1370–1378. DOI: [10.1080/25740881.2020.1738479](https://doi.org/10.1080/25740881.2020.1738479).
- [27] Sunarya, R. R.; Hidayat, R.; Radiman, C. L.; Suendo, V. Electrocatalytic Activation of a DSSC Graphite Composite Counter Electrode Using in Situ Polymerization of Aniline in a Water/Ethanol Dispersion of Reduced Graphene Oxide. *J. Electron. Mater.* **2020**, *49*(5), 3182–3190. DOI: [10.1007/s11664-020-07977-3](https://doi.org/10.1007/s11664-020-07977-3).
- [28] Reza, M.; Utami, A. N.; Amalina, A. N.; Benu, D. P.; Fatya, A. I.; Agustina, M. K.; Yuliarto, B.; Kaneti, Y. V.; Ide, Y.; Yamauchi, Y., et al. Significant Role of Thorny Surface Morphology of Polyaniline on Adsorption of Triiodide Ions Towards Counter Electrode in Dye-Sensitized Solar Cells. *New J. Chem.* **2021**, *45*(13), 5958–5970. DOI: [10.1039/D0NJ06180H](https://doi.org/10.1039/D0NJ06180H).
- [29] Doan, T. C. D.; Ramaneti, R.; Baggerman, J.; Tong, H. D.; Marcelis, A. T. M.; van Rijn, C. J. M. Intrinsic and Ionic Conduction in Humidity-Sensitive Sulfonated Polyaniline. *Electrochim. Acta.* **2014**, *127*, 106–114. DOI: [10.1016/j.electacta.2014.01.150](https://doi.org/10.1016/j.electacta.2014.01.150).
- [30] Xu, J.; Yao, P.; Li, X.; He, F. Synthesis and Characterization of Water-Soluble and Conducting Sulfonated Polyaniline/Para-Phenylenediamine-Functionalized Multi-Walled Carbon Nanotubes Nano-Composite. *Mater. Sci. Eng. B.* **2008**, *151*(3), 210–219. DOI: [10.1016/j.mseb.2008.07.003](https://doi.org/10.1016/j.mseb.2008.07.003).
- [31] Román, P.; Cruz-Silva, R.; Vazquez-Duhalt, R. Peroxidase-Mediated Synthesis of Water-Soluble Fully Sulfonated Polyaniline. *Synth. Met.* **2012**, *162*(9–10), 794–799. DOI: [10.1016/j.synthmet.2012.02.019](https://doi.org/10.1016/j.synthmet.2012.02.019).
- [32] Shimizu, S.; Saitoh, T.; Uzawa, M.; Yuasa, M.; Yano, K.; Maruyama, T.; Watanabe, K. Synthesis and Applications of Sulfonated Polyaniline. *Synth. Met.* **1997**, *85*(1–3), 1337–1338. DOI: [10.1016/S0379-6779\(97\)80260-3](https://doi.org/10.1016/S0379-6779(97)80260-3).
- [33] Narasimhan, M.; Hagler, M.; Cammarata, V.; Thakur, M. Junction Devices Based on Sulfonated Polyaniline. *Appl. Phys. Lett.* **1998**, *72*(9), 1063–1065. DOI: [10.1063/1.120965](https://doi.org/10.1063/1.120965).
- [34] Yue, J.; Epstein, A. J. Synthesis of Self-Doped Conducting Polyaniline. *J. Am. Chem. Soc.* **1990**, *112*(7), 2800–2801. DOI: [10.1021/ja00163a051](https://doi.org/10.1021/ja00163a051).
- [35] Yue, J.; Wang, Z. H.; Cromack, K. R.; Epstein, A. J.; MacDiarmid, A. G. Effect of Sulfonic Acid Group on Polyaniline Backbone. *J. Am. Chem. Soc.* **1991**, *113*(7), 2665–2671. DOI: [10.1021/ja00007a046](https://doi.org/10.1021/ja00007a046).
- [36] Huang, J. Syntheses and Applications of Conducting Polymer Polyaniline Nanofibers. *Pure Appl. Chem.* **2006**, *78*(1), 15–27. DOI: [10.1351/pac200678010015](https://doi.org/10.1351/pac200678010015).
- [37] Wei, X.-L.; Wang, Y. Z.; Long, S. M.; Bobeczko, C.; Epstein, A. J. Synthesis and Physical Properties of Highly Sulfonated Polyaniline. *J. Am. Chem. Soc.* **1996**, *118*(11), 2545–2555. DOI: [10.1021/ja952277i](https://doi.org/10.1021/ja952277i).
- [38] Doan, T. C. D.; Ramaneti, R.; Baggerman, J.; van der Bent, J. F.; Marcelis, A. T. M.; Tong, H. D.; van Rijn, C. J. M. Carbon Dioxide Sensing with Sulfonated Polyaniline. *Sens. Actuators B Chem.* **2012**, *168*, 123–130. DOI: [10.1016/j.snb.2012.03.065](https://doi.org/10.1016/j.snb.2012.03.065).
- [39] Xing, C.; Zhang, Z.; Yu, L.; Waterhouse, G. I. N.; Zhang, L. Anti-Corrosion Performance of Nanostructured Poly (Aniline-Co-Metanicilic Acid) on Carbon Steel. *Prog. Org. Coat.* **2014**, *77*(2), 354–360. DOI: [10.1016/j.porgcoat.2013.10.010](https://doi.org/10.1016/j.porgcoat.2013.10.010).
- [40] Dai, J.; Zhu, L.; Tang, D.; Fu, X.; Tang, J.; Guo, X.; Hu, C. Sulfonated Polyaniline as a Solid Organocatalyst for Dehydration of Fructose into 5-Hydroxymethylfurfural. *Green Chem.* **2017**, *19*(8), 1932–1939. DOI: [10.1039/C6GC03604J](https://doi.org/10.1039/C6GC03604J).
- [41] MacDiarmid, A. G.; Chiang, J. C.; Richter, A. F.; Somasiri, N. L. D.; Epstein, A. J. Polyaniline: Synthesis and Characterization of the Emeraldine Oxidation State by Elemental Analysis. In

- Conducting Polymers*; Alcácer, L., Ed.; Springer Netherlands: Dordrecht, 1987; pp 105–120. DOI: 10.1007/978-94-009-3907-3_9.
- [42] Reza, M.; Steky, F. V.; Suendo, V. Effect of Acid Doping on Junction Characteristics of ITO/Polyaniline/N719/Ag Diode. *J. Electron. Mater.* 2020, 49(3), 1835–1840. DOI: 10.1007/s11664-019-07906-z.
- [43] Qi, B.; Wang, J. Fill Factor in Organic Solar Cells. *Phys. Chem. Chem. Phys.* 2013, 15(23), 8972. DOI: 10.1039/c3cp51383a.
- [44] Foster, N. C. Sulfonation and Sulfation Processes. 1997, 36.
- [45] Suter, C. M.; Evans, P. B.; Kiefer, J. M. Dioxane Sulfotrioxide, a New Sulfating and Sulfonating Agent. *J. Am. Chem. Soc.* 1938, 60(3), 538–540. DOI: 10.1021/ja01270a009.
- [46] Ashar, N., and Golwalkar, K. *A Practical Guide to the Manufacture of Sulfuric Acid, Oleums, and Sulfonating Agents*; Switzerland: Springer. 2013, XIII, 146, 2013. doi:10.1007/978-3-319-02042-6.
- [47] Maas, J., and Baunack, F. Chlorosulfuric Acid. In *Ullmann's Encyclopedia of Industrial Chemistry*, Eds. Weinheim: Wiley-VCH; pp. 1–6. DOI:10.1002/14356007.a07_017.
- [48] Tanemura, K.; Suzuki, T.; Horaguchi, T. Synthesis of Sulfonated Polynaphthalene, Polyanthracene, and Polypyrene as Strong Solid Acids via Oxidative Coupling Polymerization. *J. Appl. Polym. Sci.* 2013, 127(6), 4524–4536. DOI: 10.1002/app.38045.
- [49] Yasuda, S.; Hamaguchi, E., and Asano, K. Ready Chemical Conversion of Acid Hydrolysis Lignin into Water-Soluble Lignosulfonate III: Successive Treatment of Acid Hydrolysis Lignin and a Lignin Model Compound by Phenolation and Arylsulfonation. *Journal of Wood Science.* 1999, 45, 245–249. DOI: 10.1007/BF01177733.
- [50] Sharghi, H.; Shiri, P.; Aberi, M. An Overview on Recent Advances in the Synthesis of Sulfonated Organic Materials, Sulfonated Silica Materials, and Sulfonated Carbon Materials and Their Catalytic Applications in Chemical Processes. *Beilstein J. Org. Chem.* 2018, 14, 2745–2770. DOI: 10.3762/bjoc.14.253.
- [51] Chiang, J.-C.; MacDiarmid, A. G. 'Polyaniline': Protonic Acid Doping of the Emeraldine Form to the Metallic Regime. *Synth. Met.* 1986, 13(1–3), 193–205. DOI: 10.1016/0379-6779(86)90070-6.
- [52] Cao, Y.; Li, S.; Xue, Z.; Guo, D. Spectroscopic and Electrical Characterization of Some Aniline Oligomers and Polyaniline. *Synth. Met.* 1986, 16(3), 305–315. DOI: 10.1016/0379-6779(86)90167-0.
- [53] Liao, Y.; Strong, V.; Chian, W.; Wang, X.; Li, X.-G.; Kaner, R. B. Sulfonated Polyaniline Nanostructures Synthesized via Rapid Initiated Copolymerization with Controllable Morphology, Size, and Electrical Properties. *Macromolecules.* 2012, 45(3), 1570–1579. DOI: 10.1021/ma2024446.
- [54] Li, G.; Zhang, C.; Peng, H.; Chen, K.; Zhang, Z. Hollow Self-Doped Polyaniline Micro/Nanostructures: Microspheres, Aligned Pearls, and Nanotubes. *Macromol. Rapid Commun.* 2008, 29(24), 1954–1958. DOI: 10.1002/marc.200800501.
- [55] Mazeikiene, R.; Tomkute, V.; Kuodis, Z.; Niaura, G.; Malinauskas, A. Raman Spectroelectrochemical Study of Polyaniline and Sulfonated Polyaniline in Solutions of Different PH. *Vib. Spectrosc.* 2007, 44, 201–208. DOI: 10.1016/j.vibspec.2006.09.005.
- [56] Wang, Z. H.; Javadi, H. H. S.; Ray, A.; MacDiarmid, A. G.; Epstein, A. J. Electron Localization in Polyaniline Derivatives. *Phys. Rev. B.* 1990, 42(8), 5411–5414. DOI: 10.1103/PhysRevB.42.5411.
- [57] Berner, D.; Travers, J. P.; Rannou, P. Investigation of the Ageing Effect on PANI-CSA by Conductivity and Magnetoresistance Measurements. *Synth. Met.* 1999, 101(1–3), 836–837. DOI: 10.1016/S0379-6779(98)01307-1.
- [58] Mu, S. Polyaniline with Two Types of Functional Groups: Preparation and Characteristics. *Macromol. Chem. Phys.* 2005, 206(6), 689–695. DOI: 10.1002/macp.200400408.
- [59] Zeng, X.-R., and Ko, T.-M. Structure-Conductivity Relationships of Iodine-Doped Polyaniline. 1997, 35 (13), 1993–2001. DOI: 10.1002/(SICI)1099-0488(19970930)35:13<1993::AID-POLB1>3.0.CO;2-O.
- [60] Li, Q.; Wu, J.; Tang, Q.; Lan, Z.; Li, P.; Lin, J.; Fan, L. Application of Microporous Polyaniline Counter Electrode for Dye-Sensitized Solar Cells. *Electrochem. Commun.* 2008, 10(9), 1299–1302. DOI: 10.1016/j.elecom.2008.06.029.
- [61] Kusumawati, Y.; Martoprawiro, M. A.; Pauporté, T. Effects of Graphene in Graphene/TiO₂ Composite Films Applied to Solar Cell Photoelectrode. *J. Phys. Chem. C.* 2014, 118 (19), 9974–9981. DOI: 10.1021/jp502385p.